International Journal of Mining, Reclamation and Environment

ISSN: 1748-0930 (Print) 1748-0949 (Online) Journal homepage: www.tandfonline.com/journals/nsme20

Optimising bench-level energy distribution based on drilling error measurements in the mining industry

Sean Klerkx, Masoud Soleymani Shishvan, Amin Moniri-Morad & Javad Sattarvand

To cite this article: Sean Klerkx, Masoud Soleymani Shishvan, Amin Moniri-Morad & Javad Sattarvand (2026) Optimising bench-level energy distribution based on drilling error measurements in the mining industry, International Journal of Mining, Reclamation and Environment, 40:3, 165-186, DOI: 10.1080/17480930.2025.2508820

To link to this article: https://doi.org/10.1080/17480930.2025.2508820

INTERNATIONAL JOURNAL OF MINING, RECLAMATION AND ENVIRONMENT
2026, VOL. 40, NO. 3, 165–186
https://doi.org/10.1080/17480930.2025.2508820

Optimising bench-level energy distribution based on drilling error measurements in the mining industry

Sean Klerkx[a], Masoud Soleymani Shishvan[a], Amin Moniri-Morad[b] and Javad Sattarvand[b]

[a]Department of Geosciences and Engineering, Delft University of Technology, Delft, The Netherlands; [b]Department of Mining and Metallurgical Engineering, University of Nevada, Reno, USA

ABSTRACT

Drillhole location deviations can disrupt energy distribution within mining benches, leading to uneven fragmentation and reduced operational efficiency. This study presents an optimisation approach that compensates for drilling inaccuracies to achieve more uniform energy input. The method involves discretizing the bench into a block model to estimate localised energy distribution and constructing a mathematical model to minimise discrepancies between the planned and actual energy delivery. A Tabu Search algorithm is used to solve the model. Case studies demonstrated improvements in the objective function, ranging from 0.53%–1.54% overall, and 2.14%–3.94% within the zones most affected by deviation.

ARTICLE HISTORY
Received 5 August 2024
Accepted 15 May 2025

KEYWORDS
Energy distribution optimization; fragmentation; drilling deviation analysis; metaheuristic optimization

1. Introduction

Rock fragmentation analysis is indispensable in the mining industry, leading to efficiency and productivity improvements. By examining the size distribution of blasted rock, this analysis profoundly affects the economic viability and operational effectiveness of mining operations. It is not solely about collecting data – it is a crucial strategy, guiding analysts through the complexities of rock fragmentation to drive operations towards success. Previous studies have revealed that improper blasting could lead to issues like backbreak [1,2], undesirable rock fragmentation [3,4], rockburst [5,6], flyrock [7,8], air overpressure [9,10], and blast-induced ground vibration [11–13]. The current study focuses on analysing rock fragmentation, recognising it as one of the most crucial challenges in drilling and blasting operations and its downstream implications. Various variables, including geological features [14,15] and blasting execution elements [16], exert influence on fragmentation outcomes, each playing a crucial role in shaping the size distribution of blasted rock, as demonstrated in numerous studies. In the area of geological features, Thornton et al. [17] introduced a stochastic modelling approach to assess how variables such as rock mass properties influence fragmentation outcomes during blasting. They leveraged these factors as statistical distributions and provided a representation of fragmentation. Kiliç et al. [18] examined the impact of rock mass properties on blasting efficiency, comparing intact rock characteristics with block fragmentation under similar blasting conditions. They found a strong correlation between block fragmentation and Brazilian tensile strength and internal friction angle, suggesting predictive potential for rock properties in estimating block fragmentation.

Blast pattern, as a blast execution element, determines the spatial distribution of explosives within the rock mass, influencing fragmentation, slope stability, and subsequent loading and

CONTACT Javad Sattarvand jsattarvand@unr.edu Department of Mining and Metallurgical Engineering, University of Nevada, 1664 N. Virginia Street, Reno, NV 89557, USA

hauling processes. Gebretsadik et al. [19] employed machine learning algorithms for predicting rock fragmentation, focusing on several blast pattern parameters such as spacing and burden. Results emphasised the importance of optimising blasting operations for improved efficiency and cost-effectiveness. Lan et al. [20] analysed damage mechanisms during multi-long-hole blasting with large empty holes. They found that the empty hole configurations in the blast patterns could significantly impact the rock fragmentation. Ma et al. [21] explored decoupled charge structures in rock blasting, examining their effects on failure patterns and fragmentation size distribution. They discussed the influence of delay time, initiation mode, and coupling medium on rock breakage effectiveness. Saka et al. [22] studied the impact of short burden and spacing on blasting output in open-pit mines. They found that larger burden and spacing configurations led to increased productivity and safer operations. Blast timing is another blast execution element that significantly influences fragmentation outcomes, with several studies focusing on this aspect. Omidi [23] analysed the effect of timing on blast fragmentation, concentrating on bench blasting simulations. They demonstrated that shorter inter-hole delays produced coarse fragmentation with limited backbreak, whereas longer delays resulted in finer fragmentation with heightened damage to the block's rear.

Blast size and shape are other critical blast execution elements, playing a crucial role in fragmentation outcomes. Longer blast patterns, preferably three to four times longer than wide, minimise blast boundaries, leading to better fragmentation. Multirow blasts offer advantages in productivity, though excessive rows may cause issues like inadequate fragmentation and ground vibrations [24]. Hosseini et al. [25] assessed the effect of different blast design parameters on blast operation outcomes, including the influence of blast shape. Their findings revealed that square blasts induced greater wave interference and resulted in higher peak particle velocity compared to rectangular shapes. Agrawal [26] evaluated the effects of delay timing and blast size on fragmentation outcomes. Findings revealed that fewer rows yielded larger fragments, highlighting the importance of blast size. Also, the study demonstrated that higher delay per unit burden values enhanced fragmentation and muckpile profiles, crucial in stronger sandstone formations where shorter inter-row delays are vital for better fragmentation.

Explosive material selection is another crucial blast execution element impacting fragmentation outcomes. Different explosives possess varying properties, necessitating consideration alongside geometric factors. Esen et al. [27] examined how changing explosive type affects fragmentation. Tests with ANFO and BARANFO 50 in the same case study revealed that BARANFO 50 produced finer fragmentation, indicating the importance of considering explosive performance, not just purchase price, for optimal fragmentation outcomes. Dotto and Pourrahimian [28] revealed that stronger explosives led to extensive fractures in hard rocks, while weaker alternatives offered improved energy distribution. Paswan et al. [29] analysed different blasting methods and explosive setups to enhance fragmentation results in areas with prevalent discontinuities, underscoring the necessity of accounting for explosive properties to achieve optimal fragmentation.

Drilling practice is another vital blast execution element affecting the fragmentation outcomes. Percussive and rotary drilling methods cater to different rock types and hole sizes aid geological assessment for optimised fragmentation. Recently, modern technologies, such as laser scanning and virtual reality [30] are employed as monitoring tools for the acquisition of more accurate data, such as safety, rock mass properties, rotation speed, penetration rate, depth of the hole, percussive pressure, and rotation pressure [31,32]. One such technology is Measurement While Drilling (MWD), a method used to continuously monitor the drilling process. This method is employed to estimate rock strength [33], evaluate blasthole chargeability [34], and identify rock mass discontinuities [35]. Piyush et al. [36] investigated the effect of drilling practices on fragmentation outcomes, demonstrating how even minor deviations can significantly influence results. Their study integrated advanced MWD techniques with blasting operations, aiming to enhance blasting designs and outcomes through real-time geological data acquisition. Adebayo and Mutandwa [37] investigated the impact of blast-hole deviations on fragment size and associated costs. Results indicated

a decrease in mean fragment size with increasing deviation, with ANFO explosives yielding larger fragments. Valencia et al. [38] introduced a novel method for blasthole monitoring in open-pit mines, employing aerial drone images and machine learning techniques. By processing photogrammetry [39] representations of blast patterns, the approach achieved high accuracy in blasthole detection, validating its effectiveness in optimising drilling accuracy and blasting outcomes.

As many variables impact the fragmentation outcomes, some studies have focused on optimising these variables. Vokhmin et al. [40] underscored the need to optimise drilling-and-blasting pattern parameters in their case study to improve fragmentation outcomes and minimise blasting expenses. By aligning calculation parameters with observed fragmentation, the prediction of grain-size composition could be refined, enhancing both blasting effectiveness and cost-efficiency. Afum and Temeng [41] conducted a study to optimise drill and blast operations in a gold mine, with the goal of reducing costs and enhancing efficiency. Their research involved proposing and evaluating blast geometric parameters for three operational pits, analysing their potential effects on fragmentation, explosive energy utilisation, material volume blasted, and cost savings when compared to current parameters. Ninepence et al. [42] delved into blast optimisation strategies to enhance downstream processes. Their assessment of current drill and blast parameters unveiled suboptimal fragmentation. Utilizing the Kuz-Ram Model, they proposed two optimisation options, foreseeing potential cost savings of 35.37% and 30.6%. Zhao et al. [43] created a mathematical model aimed at optimising step drilling and blasting expenses in mines, thereby improving blasting quality and reducing production costs. By refining the Gray Wolf algorithm, the model optimises drilling and blasting parameters, resulting in enhanced blasting performance and greater production efficiency. This approach was successfully applied in a limestone mine, where it led to reduced stope production costs.

The rest of the paper is organised as follows: Section 2 outlines the scope, objectives, and contributions of the study. Section 3 details the proposed methodology, including the optimisation model. Section 4 describes the case studies utilised in the research. Section 5 presents the results of the calculations from the case studies. Section 6 discusses the study' results, while Section 7 presents conclusions and key remarks.

2. Scope and objectives

In modern mining, achieving 100% precise drilling remains challenging despite the use of advanced GPS-equipped drill rigs. Various factors, such as poor setup, GPS inaccuracies, and operator inexperience, contribute to inevitable collaring deviations. Addressing these issues, the research team of the mining automation laboratory at the University of Nevada, Reno in collaboration with the Technical University of Delft have developed a comprehensive approach to minimise negative impacts of the inaccurate drilling patterns. Initially, Battulwar et al. [44] developed a practical methodology using unmanned aerial vehicles (UAVs) to create high-resolution three-dimensional models of the mine highwalls, providing a detailed visual foundation for further analysis. This method maintains aerial systems at a consistently close distance above the ground to capture high-resolution images. Building on this, Valencia et al. [38] employed these high-resolution images to automatically detect blasthole collar deviation errors from planned blast patterns using photogrammetry and computer vision techniques. These efforts aimed to identify the accuracy of blasthole placement and ensure that deviations could be practically detected.

The current study revolves around the utilisation of detected blasthole collar deviations in blast design. Specifically, this study proposes an optimal adjustment of the explosive charges based on the detected deviations to optimise the explosive energy distribution (EED), rather than uniformly charging the blastholes according to the original blast design patterns. By aligning the real EED with the designed configuration, this approach produces optimal fragmentation and enhances overall blast performance and efficiency. In the proposed approach, a sensitivity analysis is first performed using the Taguchi method to examine the impact of various blast design parameters on rock

fragmentation, backbreak, and blast vibration. This analysis informs the development of an optimisation problem to determine the optimal amount of charge in the blastholes. Given the complexity of calculating the EED, metaheuristic techniques, such as Tabu Search and Genetic Algorithm, are employed to find near-optimal solutions. These methods can adjust explosive charges in real-time, ensuring that blasts with deviated blastholes more closely resemble the original plans. The proposed approach provides a practical and innovative solution to the persistent issue of blasthole collar deviation, contributing to improved safety, efficiency, and cost-effectiveness in mining operations.

3. Materials and methods

3.1. Model development and configuration

To accurately represent the EED around blastholes, the surrounding area corresponding to the rock mass of a bench is discretized into a block model. The EED throughout the blast area is then calculated for each block using Equation 1, which is based on the three-dimensional explosive energy flux developed by [45], and then integrated and rewritten to Equation 2

$$P = \int_{L_1}^{L_2} \frac{1000 \cdot \rho_e \cdot \pi\left(\frac{D}{2}\right)^2}{\rho_r \cdot \frac{4}{3}\pi\left(h^2 + l^2\right)^{\frac{2}{3}}} dl \tag{1}$$

$$P = 187.5 \cdot \frac{\rho_e}{\rho_r} \cdot D \cdot \frac{1}{h^2}\left(\frac{L_2}{r_2} - \frac{L_1}{r_1}\right) \tag{2}$$

where L_1 and L_2 are the lengths of the explosive column above and below the elevation point P. The densities of the explosive and rock are denoted by p_e and P_r, respectively, with the rock density for limestone assumed to be 2.65 g/cm^3. The three-dimensional distances from P to the top and bottom of the column charge are indicated by r_1 and r_2, respectively. Furthermore, h represents the horizontal distance between an arbitrary point P and the blasthole, while D denotes the drillhole diameter.

Evaluating the EED formula within the block model requires multiple iterations rather than a single assessment. To assess how different charge configurations affect the distribution of explosive energy, recalculations are necessary for various blasthole arrangements and charging instructions. Consequently, each block in the model will contain data corresponding to different blasthole setups, including planned, real, and optimised EED. The planned EED reflects the EED based on the intended coordinates of the drillholes and their corresponding charging instructions. Also, the EED calculated from the real drillhole configuration is defined as the real EED. In this situation, the drillholes' coordinates deviate from the planned values, but the charging instructions remain unchanged. This represents the EED with no charge adjustments, reflecting the current state of blasting with deviated holes, without optimisation. In contrast, the optimised EED, which also uses deviated drillholes, involves adjusting the explosive charges to achieve a more favourable result. While the planned and real EED are computed only once for a given blast pattern, the optimised EED is recalculated multiple times throughout the optimisation process. For optimising charge adjustments, each blasthole is discretised based on the below guidelines:

- The coordinates of x, y, and z of the blastholes do not have to align with the block model's discretisation grid; instead, these coordinates are used as provided in the data, allowing each hole to be discretised independently on its own grid.
- The given z-coordinate sets the upper boundary of the hole, while the drilled depth determines the lower boundary. These boundaries, along with the specified height of stemming, determine the z-coordinates for the top and bottom of the explosive column.

- Charge adjustments are made in discrete segments of a specified length, which dictates the range of possible adjustment options during optimisation.
- During optimisation, the coordinates for the bottom and top coordinates of the charge modify the height of the explosive column and the amount of explosives in each hole individually.

3.2. Control parameters

Block size, search radius for calculations around each blasthole, charge segment length, and the data subset used in optimisation are identified as control parameters for which appropriate settings must be determined. The choices for block size and search radius primarily involve a trade-off between accuracy and computational requirements. While this consideration also applies to the selection of a suitable charge segment length, the charging instructions' level of detail must, above all, be practically achievable.

Significant discrepancies are observed in blocks near the blastholes as a result of comparing the block-to-block EED values for various drillhole and charging configurations. A block near the blastholes in the planned pattern may show extreme EED values, while its value drops significantly if the actual hole location is further away. To manage these unusually high values, only a subset of the EED data is considered by applying a percentile-based cap. Consequently, optimisation should primarily target areas receiving relatively low explosive energy.

3.3. Optimisation

In the developed optimisation program, the determined variables correspond to the z-coordinates for the bottom and top of the explosive columns, as indicated in expressions 3 and 4. These variables are initially set according to the z-coordinates for the charges in the actual EED drillhole configuration. During optimisation, the decision variables are modified in increments corresponding to the length of a discrete charge segment.

$$x_i^{top} \text{for} i = 1, 2, \ldots, n \in DH \tag{3}$$

$$x_i^{bottom} \text{for} i = 1, 2, \ldots, n \in DH \tag{4}$$

The proposed optimisation model seeks to closely align the EED of the actual drillhole locations with the values from the planned configuration. This is accomplished by minimising the absolute block-to-block differences between the optimised EED and the planned EED. The real EED serves as the initial solution, and it is retained in the block model to facilitate comparison with the optimised EED upon completion of the optimisation process. While the real EED and planned EED remain unchanged during the optimisation process, the optimal EED is updated with charge adjustments for several blastholes in each iteration. The EED for each block is calculated using data from the drillholes within a specified search radius. Although the z-coordinates for the bottom and top of the explosive columns are unchanged in the planned EED during optimisation process, the optimal EED is calculated using these variables. The objective function is defined by the following expression:

$$minZ = \sum_{i=1}^{DH} \sum_{j=1}^{N_p} \left| E_j^{planned}\left(DH_i^{planned}\right) - E_j^{optimized}\left(DH_i^{real}, x_i^{top}, x_i^{bottom}\right) \right| \tag{5}$$

where N_p refers to all blocks j that fall within the lower p^{th} percentile of EED values in the block model, and E is the calculated EED values, taking all drillhole information DH as input according to Equations 2 In this case, $\bar{Z}$ is the arithmetic mean of the differences between the retrieved objective values.

The optimisation model constraints are given by Constraints 6–10. Constraint 6 ensures that no charge adjustments exceed the boundaries of the blasthole. Due to physical limitations, the explosive column must not extend above the collar elevation. A similar constraint could be applied for the bottom of the hole, but in this paper, only adjustments to the top z-coordinate are considered for practicality reasons of explosive loading. Constraints 7 and 8 restrict charge adjustments to practical limits. Although significantly reducing the explosive column's height could potentially improve the objective value in certain situations, the permissible adjustment is set to half the stemming height, both above and below the original z-coordinates of the explosive column.

$$x_i^{top} \leq z_{drillhole,i}^{top,real} i = 1, 2, \ldots, n \in DH \tag{6}$$

$$x_i^{top} \leq z_{charges,i}^{top,real} + \left(z_{drillhole,i}^{top,real} - z_{charges,i}^{top,real}\right)/c_{lim} i = 1, 2, \ldots, n \in DH \tag{7}$$

$$x_i^{top} \geq z_{charges,i}^{top,real} - \left(z_{drillhole,i}^{top,real} - z_{charges,i}^{top,real}\right)/c_{lim} i = 1, 2, \ldots, n \in DH \tag{8}$$

$$\sum_{i=1}^{DH}\left(x_i^{top} - x_i^{bottom}\right) \times \pi\left(\frac{1}{2}D_i\right)^2 \times \rho_{e,i} \leq \sum_{i=1}^{DH}\left(z_{charges,i}^{top,planned} - z_{charges,i}^{bottom,planned} + \left(c_{allowance} \times l_{segment}\right)\right) \times \pi\left(\frac{1}{2}D_i\right)^2 \times \rho_{e,i} \quad i = 1, 2, \ldots, n \in DH \tag{9}$$

$$\sum_{i=1}^{DH}\left(x_i^{top} - x_i^{bottom}\right) \times \pi\left(\frac{1}{2}D_i\right)^2 \times \rho_{e,i} \geq \sum_{i=1}^{DH}\left(z_{charges,i}^{top,planned} - z_{charges,i}^{bottom,planned} - \left(c_{allowance} \times l_{segment}\right)\right) \times \pi\left(\frac{1}{2}D_i\right)^2 \times \rho_{e,i} \quad i = 1, 2, \ldots, n \in DH \tag{10}$$

where callowance controls the maximum deviation allowed from the planned quantity of explosives, c_{lim} is a selected charge height limit constant, pe is the explosive density, D represents the drillhole diameter, lsegment denotes the charge segment length, and Z denotes z-coordinates at different positions within the blastholes.

Constraints 9 and 10 limit the total amount of explosives used in the blast. To keep it equal to the planned quantity, callowance must be set to zero. However, applying this constraint from the beginning of optimisation would render all individual charge adjustments infeasible. To facilitate progress and permit adjustments, a slight deviation from the planned total explosives quantity is allowed.

3.4. Genetic algorithm approach

The EED optimisation problem is addressed using a Genetic Algorithm (GA) that employs generational evolution with elitism. In this approach, candidate solutions are represented by alterations to blasthole charging instructions. These solutions are encoded as lists of the top and bottom z-coordinates of the explosive column, forming the chromosomes, with individual hole charging specifications acting as genes. Each generation comprises a population of several candidate solutions. The initial population consists of the original charging instructions, supplemented by copies of the initial solution with randomised adjustments. For each gene, a random choice is made between reducing, increasing by one charge segment length, or making no adjustment at all. Additionally, the fitness of each candidate solution is evaluated using the objective function.

Then, the best-performing solution is retained for the next generation. The remaining candidate solutions are generated through crossover and mutation of the current population's solutions. Parent solutions are selected via tournament selection with three participants. Since each offspring requires two parents, $(population \times 2) - 2$ tournaments are conducted every generation. In this case, the cutting point for single-point crossover is randomly selected, with each parent contributing opposite segments of the chromosome. Subsequently, each gene of the offspring chromosomes is exposed to a mutation probability, allowing for a random increment or decrement by one charge segment length. This process advances to a new generation, and the described procedure is repeated until a specified number of generations have elapsed without improvement in the best solution.

3.5. Tabu search approach

While the GA excels at identifying strong global solutions, Tabu Search (TS) is more effective for local searches, targeting the optimal solution within a limited range. The TS approach generates candidate solutions by exploring direct neighbours of the current solution, starting with the original charges as the initial setup. Thus, neighbouring solutions are generated by adjusting the explosive column of a single blasthole by one charge segment length, either increasing or decreasing the z-coordinate of the bottom or top of the charge column. This process is repeated for each blasthole, producing all potential neighbours of the current solution.

Unlike the GA, the TS approach does not require evaluating the EED formula for the entire block model throughout the optimisation process. As each candidate solution involves only a single charge adjustment relative to the current one, calculation time significantly cuts down by focusing on the modified blasthole. This aim is achieved by first computing the contribution of EED in the unchanged explosive column and then removing that value from the block model. Next, the EED from the adjusted charges is added. This process is repeated for all neighbouring solutions to evaluate the objective function and identify the optimal solution, which then updates the current solution. The current solution may not always be the best solution. If no neighbouring solutions improve the current one, the option with the least detrimental impact is selected. To avoid the algorithm from quickly reversing this adjustment in subsequent iterations, a Tabu tenure of 3 iterations is implemented. This tenure helps prevent the algorithm from becoming prematurely trapped in a local optimum and promotes diversification. Practically, this approach involves exploring alternative solutions rather than reverting unfavourable adjustments. This includes making adjustments in the opposite direction in neighbouring holes to address newly introduced EED differences. Finally, the TS algorithm terminates upon detecting a repetitive loop among the 'current' solutions, signalling that no further improvements are being made. At this point, the best identified solution is taken as the result of the optimisation process. If no loop is detected, the algorithm is stopped after 100 iterations without an improvement to the best solution, providing a secondary stopping criterion.

4. Case study

This study validates the proposed algorithm using two distinct datasets, including Dataset Nevada 1 and Dataset Nevada 2. The first dataset, referred to as Nevada 1, comprises 243 drillholes arranged in a nearly square blast pattern, as illustrated in Figure 1. The average distance between these drillholes results in a spacing of 4.8 m and a burden of 4.27 m. Each drillhole has a diameter of 0.125 m and a depth of 11.5 m, with the upper 4.3 m filled with stemming. The explosive used is standard ANFO with a density of 0.9 g/cm^3. This dataset includes only the planned drillhole coordinates, with deviations introduced randomly.

The second dataset, referred to as Nevada 2, contains information about 407 drillholes in total. Because not all of these were actually drilled, a portion of these planned holes were removed, with 292 remaining. Figures 2 and 3 depict a top-down view of the planned blast pattern and the real

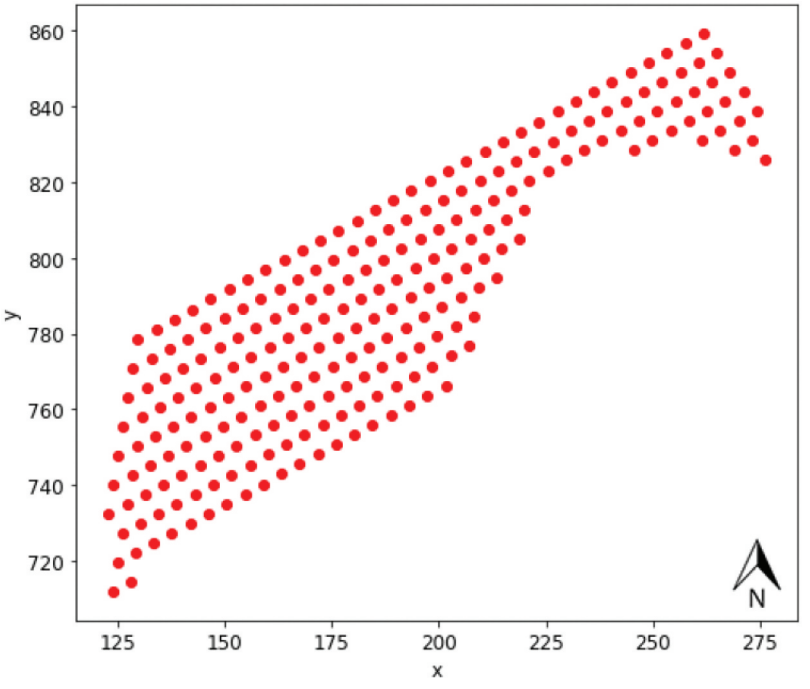

Figure 1. The locations of the planned drillholes for dataset Nevada 1, with collars at an average z-coordinate of 960 *m (x and y axes are in meters).*

drillhole locations, respectively. After conversion from imperial to metric units, a designed spacing of 5.18 *m* and burden of 4.57 *m* are obtained. The hole depth is 13.72 *m*, with drillhole diameter of 0.200 *m* and a stemming height of 4.27 *m*. Based on accessory data, an explosive density of 0.9 g/cm^3 can be derived, which is assumed to be ANFO.

The real drillhole locations were logged by the drill rigs with two decimals precision. Although this does not take into account any GPS-related inaccuracies, for the purpose of this research it serves as good data to test the application of the EED optimisation system on a blast pattern containing real deviations. Figure 4 shows a histogram of the calculated deviations, which are also plotted on a precision map in Figure 5. The deviation of six holes exceeded three times the hole diameter. For a more detailed presentation of the lesser deviations, these have been excluded from the figures. A total of 26 holes are deviated by more than one hole diameter (0.200 *m*) and are thus considered inaccurately drilled [46]. Figure 6 indicates the 5 by 5 test pattern planned drillhole locations in this study. This test pattern is utilised as a small blast pattern to identify appropriate values for the critical control parameters.

5. Results

5.1. Control variables

To avoid lengthy computation times in early testing to determine appropriate values for the control parameters, a stepwise approach was taken in which scale and resemblance to real blasthole data is progressively increased (Figure 7). This procedure improves the understanding of the involved variables before applying the method at full scale. Ultimately, it aims to ensure more consistent performance with the selected optimisation settings and control parameters, while also validating findings from earlier stages.

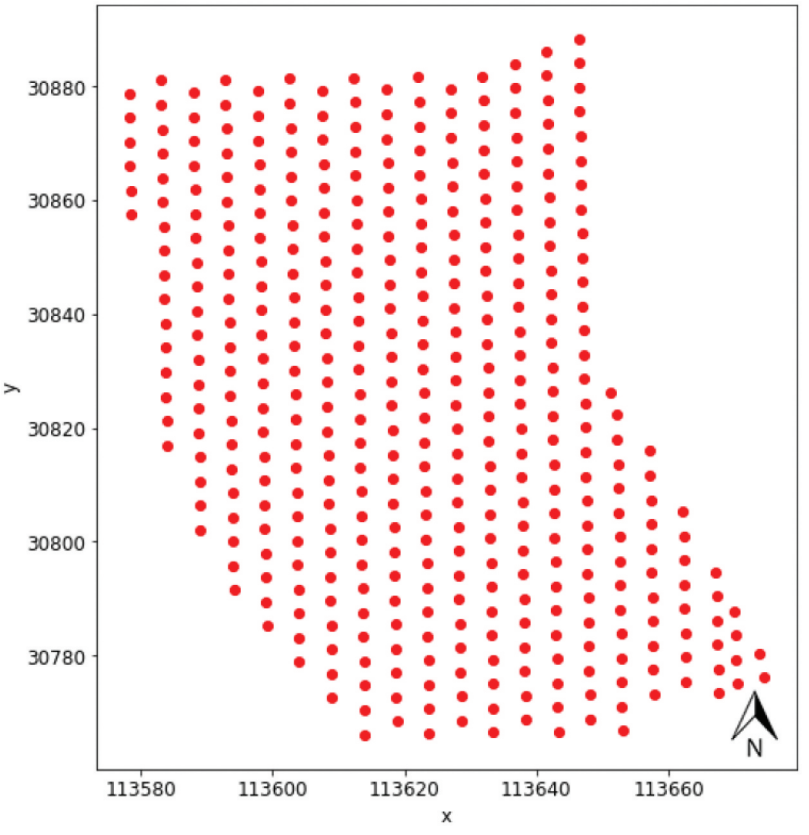

Figure 2. The locations of the planned drillholes for dataset Nevada 2, with collars at an average z-coordinate of 1633.73 *m (x and y axes are in meters).*

5.2. Search radius

Selecting a proper search radius around blastholes is crucially dependent on how the explosive energy attenuates with distance. This attenuation is governed by the EED formula established by Kleine et al. [45] and the specific characteristics of the blast. The EED around a single blasthole is evaluated to find a suitable search radius. The test blastholes reviewed have characteristics that are consistent with those of the blastholes in the Nevada 1 and Nevada 2 datasets. In this case, the EED is computed for a 20 $m \times 20$ m square block model centred around a blasthole, using a search radius (r) of 10 m. Figure 8 indicates a vertical cross-section of the EED surrounding a blasthole from Dataset Nevada 1, with the following specifications: diameter = 0.125 m, total hole depth = 11.5 m, stemming = 1.5 m, and ANFO explosive with a density of 0.9 g/cm^3.

The EED values do not follow a normal distribution, making it impractical to determine the extent of statistically significant values using the three-sigma rule based on the mean and standard deviation. Alternatively, the EED values at different radii around the blasthole are compared to the peak values observed in close proximity. This comparison helps identify the radius at which explosive energy sufficiently diminishes, allowing values outside this range to be disregarded. Moreover, since the minimum distance to the explosive column is tremendously influenced by the block size, the magnitude of the peak EED values is also affected. Furthermore, the EED values at different radii are compared to those measured at a distance of 0.5 m, at the depths where the EED is maximum. For both datasets, the optimal search radius was found to be 5.0 m, as the EED at this distance drops to 0.71% (Nevada 1) and 0.65% (Nevada 2) of the value at 0.5 m.

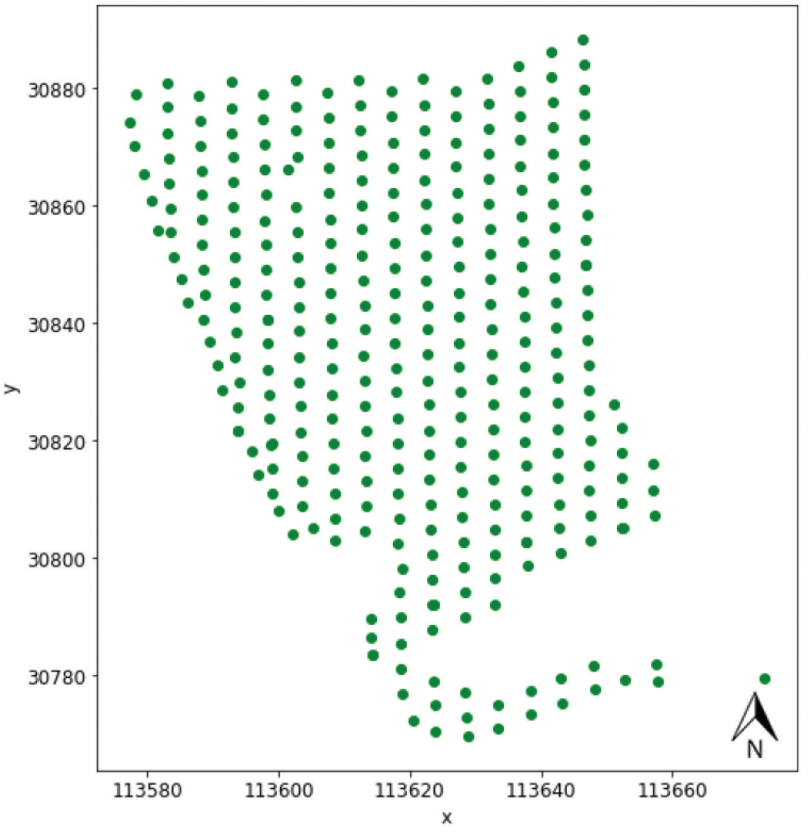

Figure 3. The locations of the real drillholes for dataset Nevada 2, with collars at an average z-coordinate of 1633.73 *m (x and y axes are in meters).*

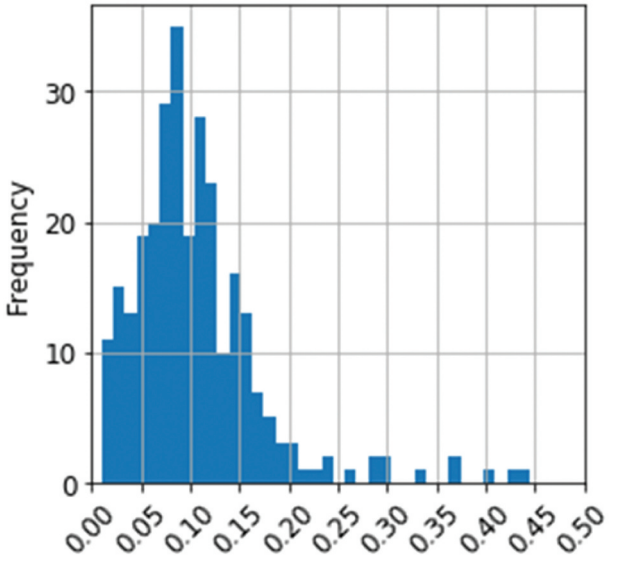

Figure 4. Frequency distribution of drillhole deviations (X axis is based on meters).

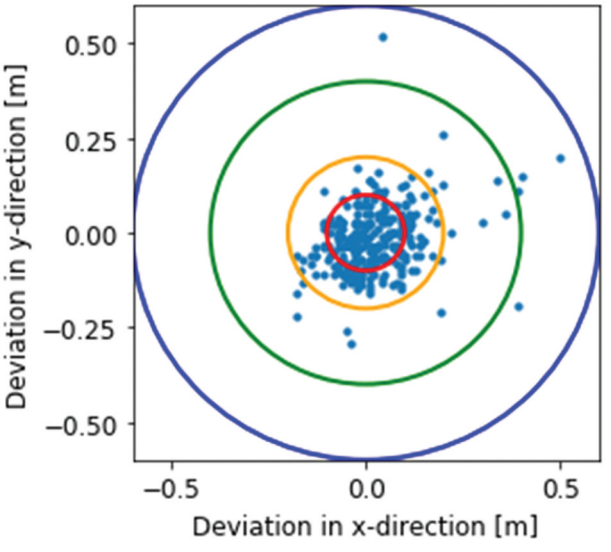

Figure 5. Drilling precision map for ½, 1, 2, and 3 times hole diameter.

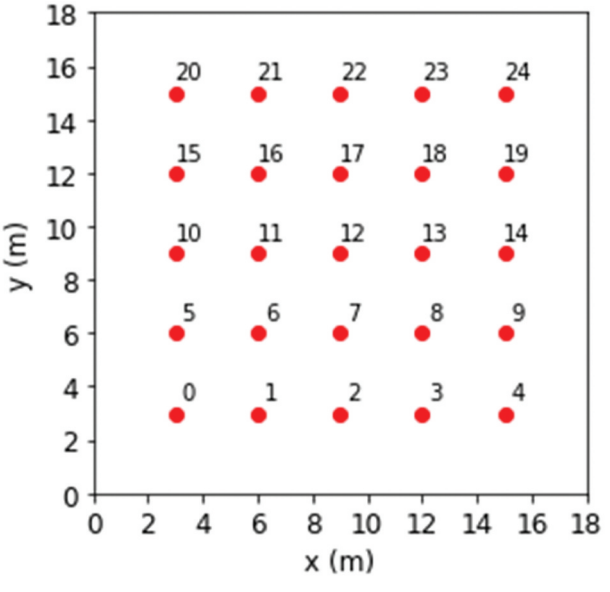

Figure 6. The 5 by 5 test pattern planned drillhole locations.

5.3. The 5 by 5 test pattern

To investigate the optimisation approach in a controlled and replicable environment, a 5 by 5 test pattern was established, consisting of 25 drillholes, each with a diameter of 0.125 *m*, arranged in a square grid. This small-scale pattern was designed to serve as a representative subset of a full blast pattern, allowing for focused analysis and parameter calibration. The planned collar coordinates were spaced evenly (3 *m*) (Figure 6), and deviations were applied based on actual field data to simulate realistic inaccuracies. Among the 25 drillholes, 12 holes displayed deviations that exceeded one hole diameter (0.2 *m*), providing sufficient variability to test the optimisation method's sensitivity and effectiveness. In this scenario, the holes expected

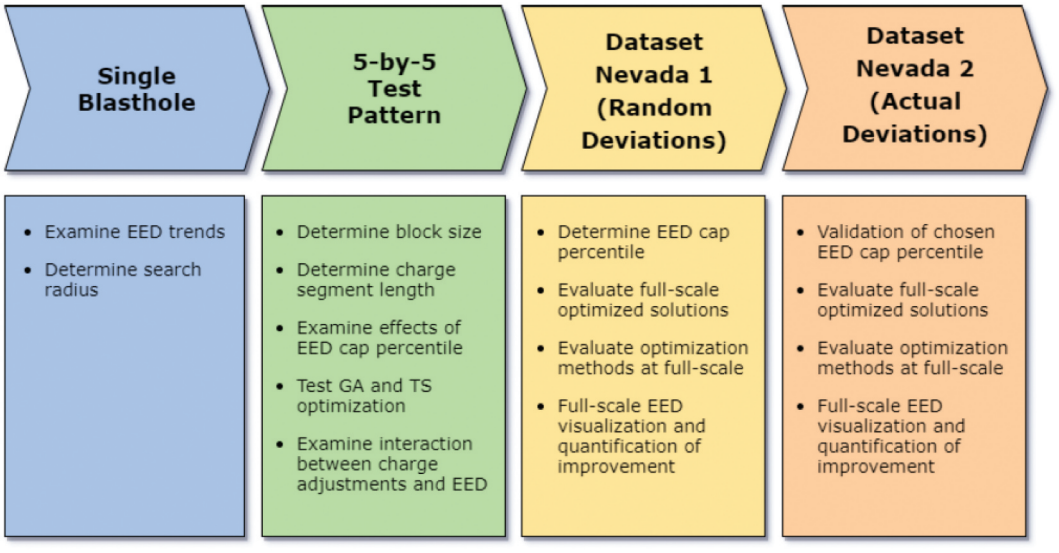

Figure 7. Detailed flowchart outlining the experimental design and objectives for each stage.

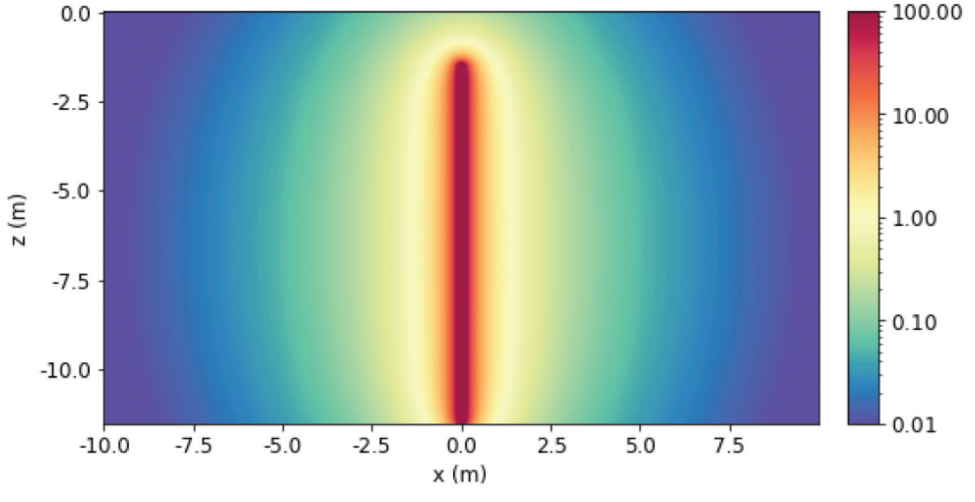

Figure 8. Vertical cross-section of the EED surrounding a blasthole in dataset Nevada 1.

to undergo explosive columns adjustments are easily identifiable, enabling a straightforward evaluation of optimisation performance. Specifically, bringing holes 1, 5, 7, 11, 13, 17, 19, and 23 closer together requires reducing the charges in holes 6 and 18 to compensate for the increased explosive energy. On the contrary, charge reductions are expected in holes 8 and 16 due to the enhanced spacing between holes 3, 7, 9, 11, 15, 17, and 21, which results in decreased explosive energy in the intervening areas.

The test pattern was especially useful in identifying appropriate values for critical optimisation parameters such as the EED cap percentile and block size. By isolating the optimisation process within this smaller array, we could monitor changes in the objective function (i.e. the total block-to-block EED difference) in response to different charge adjustment strategies. This controlled setup enabled a deeper understanding of the impact of individual deviations and the algorithm's ability to compensate for them.

Furthermore, using a smaller pattern allowed us to perform multiple simulation iterations efficiently, adjusting input conditions and validating the stability of the optimisation outcomes. It also provided a framework to test scalability before applying the methodology to full-scale datasets, such as those from Nevada 1 and 2. The insights from this phase were foundational in tuning the optimisation approach for broader application.

5.4. Block size

Block size is a critical parameter in the optimisation process, as it determines the spatial resolution at which Explosive Energy Distribution (EED) values are compared between the planned and actual drillhole configurations. A finer block size enables a more detailed representation of EED, capturing localised deviations more precisely. However, this comes at the cost of significantly increased computational demand. On the other hand, coarser block sizes reduce computational load by simplifying the problem, but may fail to detect subtle yet important variations in energy placement.

Directly comparing EED statistics across different block sizes can be misleading, as finer blocks naturally tend to yield higher mean EED values due to increased spatial granularity. As a more reliable alternative, the absolute differences between the planned EED and a manually optimised EED (which accounts for expected charge adjustments) are compared against the differences between the planned and real EED. This approach better reflects the effectiveness of optimisation in improving energy distribution.

While the block model does not need to preserve identical EED statistics across various block sizes, it should support consistent and meaningful charge adjustments. To evaluate this, various block sizes were tested on the 5 by 5 test pattern to assess their impact on optimisation outcomes. Results indicated that smaller block sizes generally resulted in lower mean block-to-block EED differences, demonstrating improved fidelity in charge allocation. However, excessively small blocks led to considerable increases in computation time and risked overfitting to localised noise.

Figure 9 illustrates the impact of block size on the improvement in mean EED difference, based on a charge segment length of 0.3 *m*. To ensure that a block size accurately reflects the EED, improvements should closely align with those observed for the smallest block sizes across each EED cap percentile. Larger discrepancies can impact the effectiveness of charge adjustments and may lead to different optimisation outcomes. The block sizes of 1.0 *m* and 0.5 *m* appear to lack precision, as evidenced by substantial discrepancies when compared to graphs of smaller block sizes. However, the improvements computed for the block sizes of 0.2, 0.1, and 0.05 *m* are quite similar, differing by only 0.04–0.17% between subsequent block sizes. Therefore, it is anticipated that the optimisation model will generate similar charge adjustments across these smaller block sizes. Also, Figure 9 illustrates that an EED cap percentile of 100%, meaning all data is used, does not yield a positive improvement in the objective value for this idealised test pattern. Therefore, these expected adjustments would never be recommended through optimisation unless a lower EED cap percentile is used. High EED values that produce disproportionately large differences between optimised and planned configurations must be limited using appropriate cap percentiles to ensure practical and effective charge adjustments.

5.5. Charge segment length

By investigating optimisation solutions for various EED cap percentiles and charge segment lengths, it becomes clear that charge reductions and charge increases do not lead to the same improvements to the objective value, even in the idealised 5 by 5 test patterns. This can lead to a bias in adjustments, as the total amount of explosives is not restricted to the quantity used in the planned configuration. Although the implementation of constraints 9 and 10 could easily mitigate this problem here, it is crucial to reduce the effect of this bias as much as possible to prevent complications in full-scale optimisation. One effective

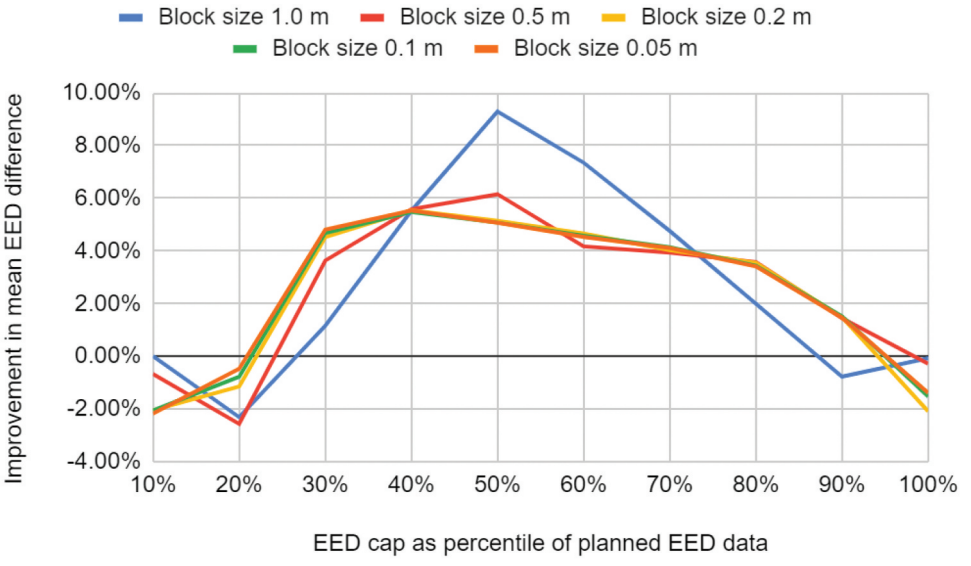

Figure 9. Comparison of improvements for different block sizes, for expected manual adjustments by 0.3 m.

approach is to use a larger charge segment length, which reduces the sensitivity of optimisation to minor EED differences. When larger EED variations are needed to effect charge adjustments, the discrepancy between increases and reductions becomes less significant. With a charge segment length of 0.3 *m*, most optimisation solutions result in an equal number of charge decrements and increments. Naturally, a charge segment length of 0.3 *m* also has improved practicality over a length of 0.1 or 0.2 *m* but maintains sufficient sensitivity to differences in EED.

5.6. EED cap percentile

In the 5 by 5 test pattern, the optimisation solutions revealed that the relationship between charge reductions and increases varies with the selected EED cap percentile. Although a charge segment length of 0.3 *m* effectively mitigates biases in this idealised scenario, its behaviour differs in non-idealised blast patterns. Optimisation of Dataset Nevada 1, with deviations randomly drawn from a uniform distribution ranging from – 0.5–0.5 *m* (0.37 *m* mean), reveals that charge reductions are favoured at high EED cap percentiles and charge increases at low values of this control parameter, as given in Table 1. After additional investigation, the EED cap percentile of 50% appears most effective at approximating a balance between charge reductions and increases.

5.7. Optimisation

Although both the GA and TS can reach the same optimal solutions, the computation times for GA are significantly longer. TS was expected to be favoured for optimisation of the 5 by 5 test cases because these generally involve a relatively small number of charge adjustments, benefiting the local search approach. However, as Figure 10 shows, GA does not outperform TS at any stage of optimisation for dataset Nevada 1 despite the fact that charge adjustments are recommended in 80 out of the 243 blastholes in the optimal solution, in which the total amount of explosives used is limited using constraints 9 and 10.

Despite the substantial number of charge adjustments, the GA does not show any advantage over the TS, even in the initial generations. With a population size of 20 and a mutation probability of

Table 1. Number of adjustments by charge segment length of 0.3 *m* for dataset Nevada 1.

EED Cap Percentile (%)	Charge Reductions	Charge Increases	Balance
10	65	47	−18
20	67	144	+77
30	51	63	+12
40	38	41	+3
50	40	41	+1
60	43	39	−4
70	49	31	−18
80	54	26	−28
90	58	8	−50
100	557	1	−556

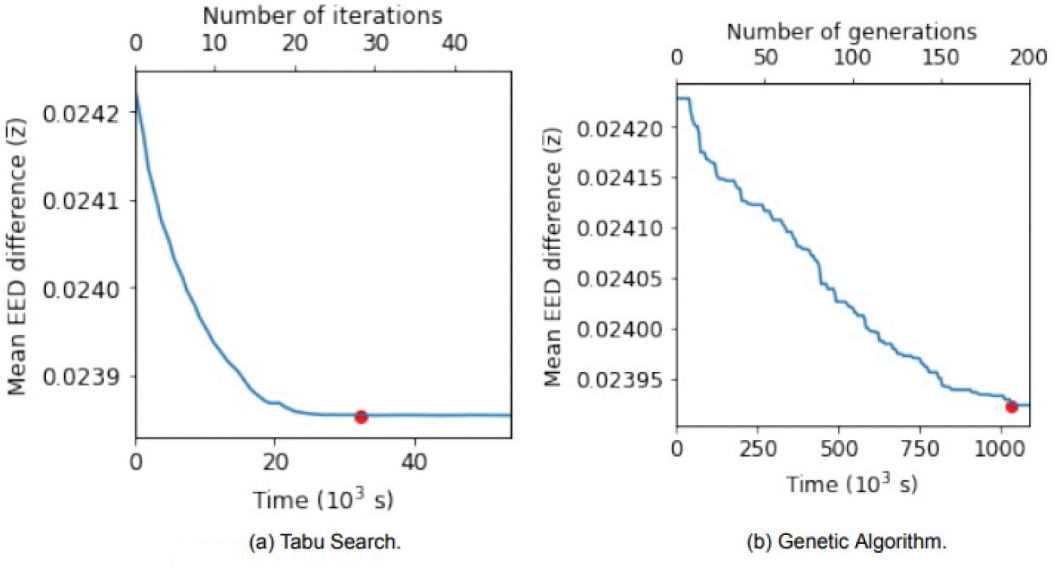

Figure 10. TS and GA optimisation path for Nevada 1 dataset (red dots indicate the best solution found).

0.005, it required almost 12.4 h to achieve the first marginal improvement, approaching the total computation time required by TS. To address the time-consuming nature of identifying the final beneficial charge adjustments, the termination criterion was adjusted to end after ten consecutive iterations without improvement. Even with this change, the computation time for this setup was 12.6 days, and the resulting solution was slightly inferior to that obtained with TS. The GA's solutions appear too random to match the effectiveness of TS's more heuristic approach. Therefore, using GA to generate a better initial solution for TS would only increase computation times, making TS alone a more efficient choice than any hybrid method.

5.8. Charge adjustment solutions

While 80 recommended charge adjustments for the Nevada 1 dataset is not necessarily excessive, a more detailed look into the functioning of the optimisation program can be provided by reducing the magnitude of the drillhole deviations to an average value of 0.19 *m*. This value was randomly selected from a uniform distribution ranging from – 0.25–0.25 *m*. This reduces the total number of charge adjustments to 20 (10 increases and 10 decreases). Though there was one exception in the previous case, no blasthole is adjusted more than once in the optimal solution, as shown in Figure 11

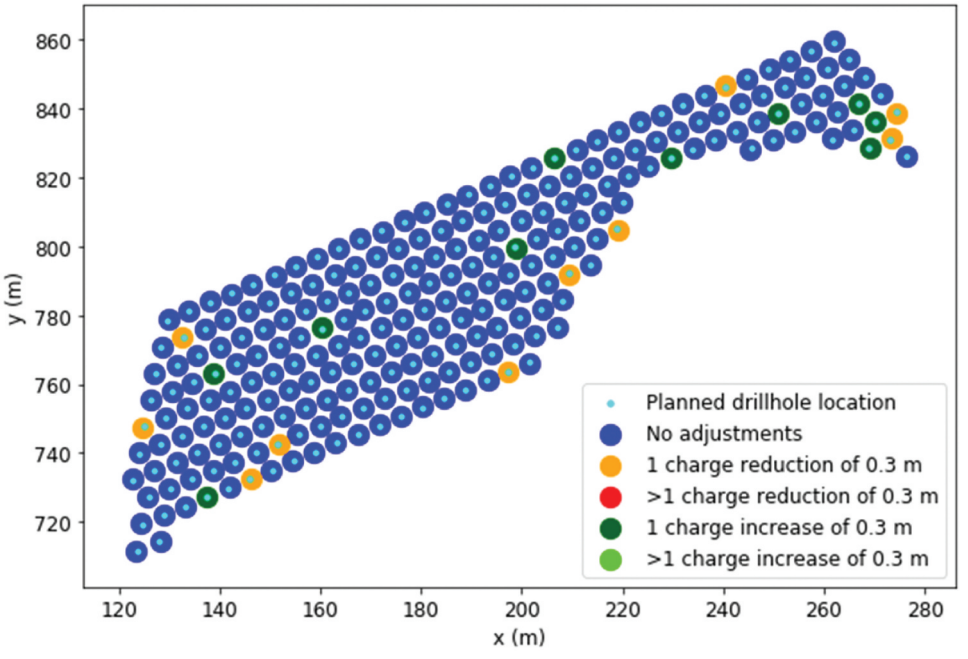

Figure 11. Charge adjustment solution for Nevada 1 dataset with smaller deviations.

In this case, most adjustments are made independently, except for a cluster in the top-right corner of the blast. This suggests minimal interaction between individual adjustments, indicating that the influence of the tabu mechanism is restricted. Another observation reveals that most charge adjustments, especially reductions, occur in drillholes at the outer boundaries of the blast pattern. Additionally, the investigation shows that 2 out of the 10 charge reductions are located just one row inward, while the remaining 8 are found in the outermost holes. Blastholes at the boundaries have one 'open' side without neighbouring blastholes to balance small increases or decreases in EED, potentially leading to larger discrepancies and thus a higher need for charge adjustments compared to areas with more surrounding blastholes.

The solution obtained for dataset Nevada 2 features a total of 7 charge adjustments (Figure 12). Once again, many of these are found at the boundaries of the blast. Nevertheless, irregular drilling at the southern and western ends of the blast has resulted in numerous significantly deviated drillholes in these boundary areas, which often require adjustments. In this case, the magnitude of deviations appears to be the primary driver for charge adjustments, rather than merely the drillhole's position at the edge of the blast pattern.

Analysis of drillholes with deviations of one diameter or more reveals that charge increases are applied to holes 6264, 6330, and 6184, while charge decreases are implemented in holes 6275, 6341, and 6342. It is clear that charge adjustments are not solely based on the degree of deviation; of the 26 drillholes with deviations exceeding the threshold of one diameter (0.200 m), adjustments were made in only 6 cases. Moreover, large deviations alone do not guarantee that charge adjustments will be made, as adjustments are also influenced by the positions of nearby drillholes. Conversely, large deviations are not always necessary for charge adjustments. For example, the study indicates that 8 out of the 14 adjustments occur in drillholes with deviations of less than one drillhole diameter. A notable instance is the cluster of adjustments in the core of the blast pattern, where a single highly deviated drillhole prompts both charge increases and decreases in surrounding holes that are otherwise positioned relatively accurately. Figure 13 indicates how the charge adjustments recommended by optimisation alter the EED values throughout the block model. Comparing the

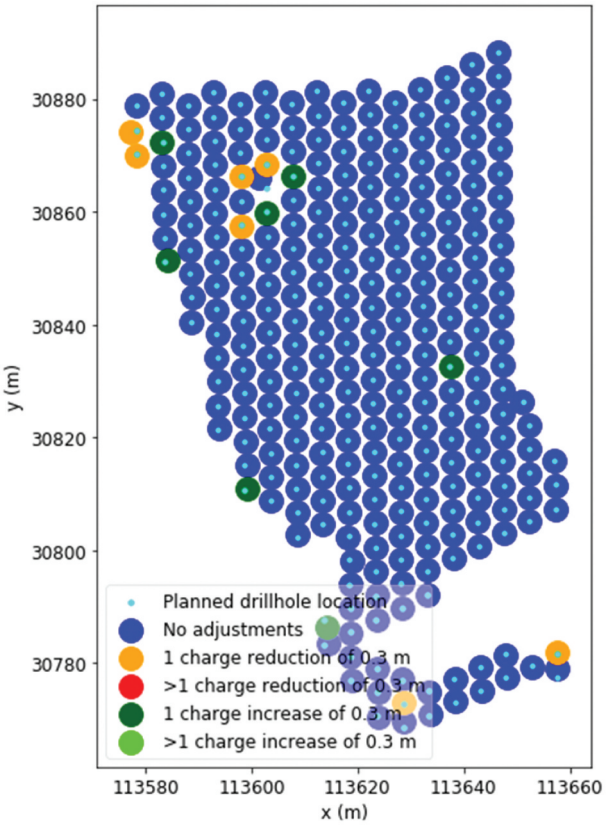

Figure 12. Charge adjustment solution for Nevada 2 dataset.

preliminary and optimised states of the EED differences highlights both the negative and positive impacts of the optimisation process. The magnitude of the newly introduced differences (red) is generally larger than the reductions (blue), although they tend to cover smaller areas. In contrast, the reductions in EED differences often extend over larger areas. Despite the localised nature of the new differences, the extensive reductions in three-dimensional space usually result in overall improvements.

The achieved improvements in the objective value are listed in Table 2 for both the Nevada 1 and Nevada 2 datasets. It is crucial to note that the objective function is computed based on differences across the whole block model. Since charges in the majority of drillholes remain unchanged, a significant portion of the EED differences remains unresolved. As a result, focusing solely on the blocks impacted by the charge adjustments recommended by the optimisation model provides a more informative representation for this scenario.

6. Discussion

While drillhole deviation is recognised as a common issue in the mining industry, its potential impact on blast performance is frequently accepted as an unavoidable margin of error. Despite advances in positioning and automation technologies, completely eliminating this problem remains challenging. Adjusting other parameters within a blast pattern that includes deviated drillholes can help align blast performance more closely with the expectations set by the original design. Given the ripple impact of fragmentation on subsequent

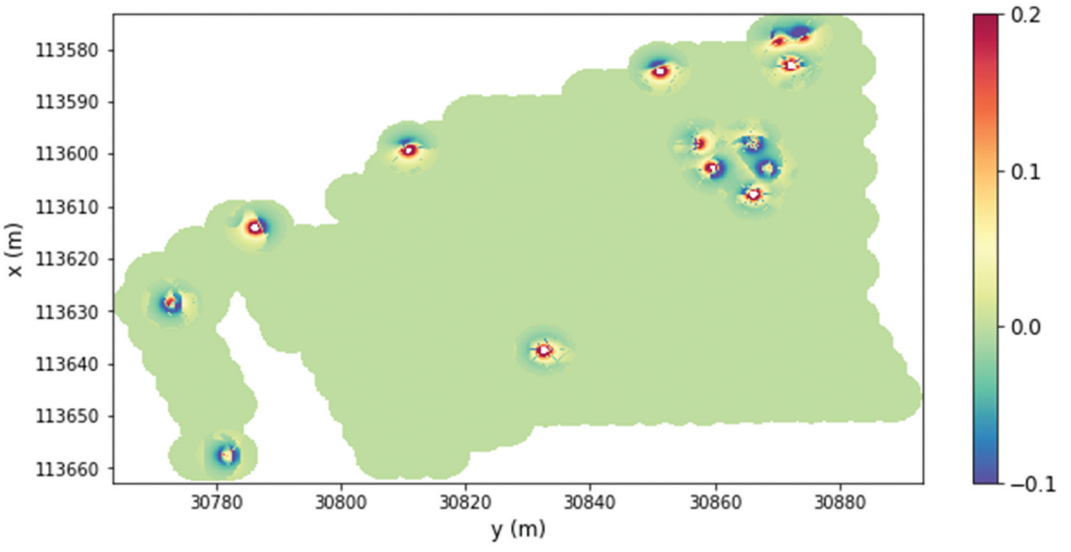

Figure 13. Differences between preliminary and optimized states of EED differences, 3.0 m below bench surface.

Table 2. Improvements achieved by optimisation.

Dataset	Improvement in the affected blocks only (%)	Improvement in the objective value (%)
Nevada 1 (large deviations)	2.31	1.54
Nevada 1 (small deviations)	2.14	0.53
Nevada 2	3.94	0.96

mining procedures, such adjustments can yield significant improvements in both efficiency and cost-effectiveness.

The decision to focus on minimising block-to-block EED value differences between the real and planned drillhole configurations has proven more challenges than initially anticipated. This choice stems from the limited understanding of EED behaviour in a blast and its subsequent impact on rock mass. While the EED formulation developed by Kleine et al. [45] offers a valuable estimate of the energy delivered at each point, the relationship between this energy and blast performance remains uncertain. Without a generalised method to correlate EED values with fragmentation predictions, a straightforward value-based approach proves inadequate. Consequently, the EED values from the real drillhole pattern can only be effectively assessed by comparing them with the planned EED values.

An unintended outcome of the block-to-block method is that drillhole deviations introduce differences in the blocks near the real and planned drillhole locations, even though the overall frequency distribution of EED values may remain unchanged. While the implementation of an EED cap addresses the largest differences, it can nevertheless impact the smaller values. For instance, if all drillholes were uniformly displaced by the same distance in the same direction, the total energy distribution across the blast should theoretically remain consistent, with the exception of changes at the designed boundaries. However, the block-by-block method will not permit the interchange of block values, leading to numerous discrepancies that must be minimised. While maintaining constant block values at the blast pattern boundaries is essential to achieve the intended rock fragmentation, the interchange of values further from the blast centre is less likely to affect overall blast performance significantly. Consequently, the current setup, which views these interchanges as detrimental to the objective, may underestimate the true improvements to the EED.

When evaluating optimality, the significance of the chosen EED cap percentile cannot be overlooked. As the results indicate, varying this parameter – an inherent aspect of the block-to-block comparison approach – yields significantly different charge adjustment solutions. Although the EED cap percentile was selected to align the optimised explosives quantity with the planned quantity and reduce bias, assessing the true optimality of these solutions remains challenging. However, the consistent performance observed in the Dataset Nevada 1 and Dataset Nevada 2, regardless of the magnitude of drillhole deviations, supports the effectiveness of the chosen percentile. In all cases examined, the optimisation process behaved as predicted, and the 50% EED cap resulted in manageable changes in explosives quantities, demonstrating its appropriateness in avoiding excessive alterations.

In the majority of TS optimisation trials performed on the 5 by 5 pattern, it was observed that the choice of tabu tenure had a negligible effect on the final outcome. While there were a few exceptions, the final solutions were generally consistent across different tabu tenure settings. The primary difference observed was that a larger tabu tenure allowed the search to explore further from local optima, but it also increased the time required to meet the stopping criterion and determine a solution as optimal. To mitigate this issue, adjusting the stopping criterion could help reduce the optimisation duration. Nonetheless, the overall computation time, which can extend to several hours, remains a major drawback.

In addition to improving EED differences, charge adjustments can introduce new variations in nearby blocks. Although these adjustments clearly benefit the surrounding area, they can also significantly alter the energy received by blocks close to the explosive column. An alternative approach to compensating for changes in explosive energy distribution might involve varying the explosive density rather than the explosive column height. If the mine site offers different types of explosives, this could be a viable option. Such an approach would influence the entire length of the blasthole, not just the area around charge height adjustments. Additionally, adjusting explosive density could minimise the impact on the shallowest parts of the blast, potentially reducing the risk of flyrock compared to altering the explosive column and stemming height.

The charge adjustment solutions derived from Dataset Nevada 1 and Dataset Nevada 2 highlight that optimising explosive charges in a specific pattern cannot rely solely on the magnitude of drillhole deviations. Although significant charge adjustments are often observed in highly deviated holes, this is not always necessary; deviations in a single drillhole do not always necessitate a large adjustment to its explosive column height. The findings indicate that interactions among multiple slightly deviated neighbouring drillholes can produce substantial EED differences. Therefore, while it might be beneficial to initially focus on potential adjustments around highly deviated holes, as opposed to the current TS algorithm's approach of evaluating all possible adjustments throughout the pattern, it is crucial not to overlook the influence of less deviated drillholes.

While the optimisation programme proves effective within the context of Nevada's blasting practices, its transferability to other locations needs careful consideration of geological, environmental, and regulatory factors. Moreover, differences in local regulations, rock characteristics, and community sensitivities may mandate significant adjustments to the programme's control parameters to ensure safe and efficient blasting practices in diverse geographic settings.

7. Conclusions

The EED optimisation system developed in this study demonstrated that adjusting the length of explosive charges could effectively mitigate the impact of drillhole deviations. Applying this optimisation to real-world case studies with the developed model achieved improvements ranging from 0.53% to 1.54%, or 2.14% to 3.94% when excluding areas not affected by the suggested charge adjustments. The approach consistently created positive outcomes across two different blast patterns, regardless of design characteristics, and was effective for both random and real drillhole deviations. The study has also successfully met several additional objectives. By maintaining

a constant quantity of used explosives across the solutions, the model theoretically enables more efficient utilisation of explosive materials. Adjusting the explosive column height seems rationally feasible in the standard procedures. The modifications to the initial blasting plan are minimal, and the proposed minimum adjustment length of 0.3 metres should be enough for operators to implement effectively. The computation time required for optimisation model was a notable concern in this study. While the TS algorithm delivered optimal solutions significantly faster than the GA and was generally found to be more suitable, its runtime of several hours remains inconvenient. To advance this research, it is suggested to explore other techniques beyond the block-to-block comparison of EED values, as any changes in block values are automatically considered undesirable differences. Alternative optimisation objective functions may better capture the true benefits. Additionally, it is crucial to evaluate the safety implications of enhancing explosive column heights at the expense of stemming, particularly regarding the flyrock risk. For future research, we recommend expanding the methodology to incorporate additional field data from diverse geological and operational contexts. This includes collecting and utilising angle deviation measurements where available and considering more influential factors such as rock mass heterogeneity, dynamic blast loading response, and explosive product characteristics. Applying the model across a broader set of blasts will also help assess its scalability and generalisability beyond the initial case studies.

Disclosure statement

No potential conflict of interest was reported by the author(s).

Funding

This study was based in part on research funded by the National Institute for Occupational Health and Safety (NIOSH) through the Capacity Building in Artificially Intelligent Mining Systems capacity (AIMS) under contract number [75D30119C06044]. The authors' opinions, findings, conclusions, and recommendations do not reflect the views of NIOSH.

ORCID

Javad Sattarvand http://orcid.org/0000-0002-9364-8775

References

[1] S. Kumar, A.K. Mishra, and B.S. Choudhary, *Prediction of back break in blasting using random decision trees*, Eng. Comput. 38 (Suppl 2) (2022), pp. 1185–1191. doi:10.1007/s00366-020-01280-9.
[2] M. Sharma, H. Agrawal, and B.S. Choudhary, *Multivariate regression and genetic programming for prediction of backbreak in open-pit blasting*, Neural Comput. Appl. 34 (3) (2022), pp. 2103–2114.
[3] M. Monjezi, A. Bahrami, and A.Y. Varjani, *Simultaneous prediction of fragmentation and flyrock in blasting operation using artificial neural networks*, Int. J. Rock Mech. Min. Sci. 47 (3) (2010), pp. 476–480. doi:10.1016/j.ijrmms.2009.09.008.
[4] P. Kulatilake, W. Qiong, T. Hudaverdi, and C. Kuzu, *Mean particle size prediction in rock blast fragmentation using neural networks*, Eng. Geol. 114 (3–4) (2010), pp. 298–311. doi:10.1016/j.enggeo.2010.05.008.
[5] Y. Pu, D.B. Apel, V. Liu, and H. Mitri, *Machine learning methods for rockburst prediction-state-of-the-art review*, Int. J. Min. Sci. Technol. 29 (4) (2019), pp. 565–570. doi:10.1016/j.ijmst.2019.06.009.
[6] A.C. Adoko, C. Gokceoglu, L. Wu, and Q.J. Zuo, *Knowledge-based and data-driven fuzzy modeling for rockburst prediction*, Int. J. Rock Mech. Min. Sci. 61 (2013), pp. 86–95. doi:10.1016/j.ijrmms.2013.02.010.
[7] M. Hasanipanah and H. Bakhshandeh Amnieh, *A fuzzy rule-based approach to address uncertainty in risk assessment and prediction of blast-induced flyrock in a quarry*, Nat Resour Res. 29 (2) (2020), pp. 669–689. doi:10.1007/s11053-020-09616-4.

[8] M.S. Barkhordari, D.J. Armaghani, and P. Fakharian, *Ensemble machine learning models for prediction of flyrock due to quarry blasting*, Int J Environ Sci Technol 19 (9) (2022), pp. 8661–8676. doi:10.1007/s13762-022-04096-w.
[9] R. Zhang, Y. Li, Y. Gui, and J. Zhou, *Prediction of blasting induced air-overpressure using a radial basis function network with an additional hidden layer*, Appl. Soft Comput. 127 (2022), pp. 109343. doi:10.1016/j.asoc.2022.109343.
[10] M. Hasanipanah, D. Jahed Armaghani, H. Khamesi, H. Bakhshandeh Amnieh, and S. Ghoraba, *Several non-linear models in estimating air-overpressure resulting from mine blasting*, Eng. Comput. 32 (3) (2016), pp. 441–455. doi:10.1007/s00366-015-0425-y.
[11] Y. Azimi, S.H. Khoshrou, and M. Osanloo, *Prediction of blast induced ground vibration (BIGV) of quarry mining using hybrid genetic algorithm optimized artificial neural network*, Measurement 147 (2019), pp. 106874. doi:10.1016/j.measurement.2019.106874.
[12] G. Paneiro and M. Rafael, *Artificial neural network with a cross-validation approach to blast-induced ground vibration propagation modeling*, Underground. Space 6 (3) (2021), pp. 281–289. doi:10.1016/j.undsp.2020.03.002.
[13] C.K. Arthur, V.A. Temeng, and Y.Y. Ziggah, *Soft computing-based technique as a predictive tool to estimate blast-induced ground vibration*, J. Sustain. Min. 18 (4) (2019), pp. 287–296. doi:10.46873/2300-3960.1115.
[14] M. Z. Abu Bakar, S. M. Tariq, M.B. Hayat, M. K. Zahoor, M. U. Khan, *Influence of geological discontinuities upon fragmentation by blasting*, Pak. J. Sci. 65 (3) (2013), pp. 414–419.
[15] E.F. Salmi and E.J. Sellers, *A review of the methods to incorporate the geological and geotechnical characteristics of rock masses in blastability assessments for selective blast design*, Eng. Geol. 281 (2021), pp. 105970. doi:10.1016/j.enggeo.2020.105970.
[16] W.A. Hustrulid, *Blasting Principles for Open Pit Mining*, 1, Netherlands: Balkema, 1999.
[17] D. Thornton, S.S. Kanchibotla, and I. Brunton, *Modelling the impact of rockmass and blast design variation on blast fragmentation*, Fragblast 6 (2) (2002), pp. 169–188. doi:10.1076/frag.6.2.169.8663.
[18] A.M. Kılıç, E. Yasar, Y. Erdoan, and P.G. Ranjith, *Influence of rock mass properties on blasting efficiency*, Sci. Res. Essay 4 (11) (2009), pp. 1213–1224.
[19] A. Gebretsadik, "*Enhancing rock fragmentation assessment in mine blasting through machine learning algorithms: A practical approach*, Discov. Appl. Sci. 6 (5) (2024), pp. 223. doi:10.1007/s42452-024-05888-0.
[20] R. Lan, R. Cheng, Z. Zhou, L. Chen, P. Wang, and Z. Wang, *Damage and fragmentation of rock under multi-long-hole blasting with large empty holes*, Rock. Mech. Rock. Eng. 57 (9) (2024), pp. 7603–7622. doi:10.1007/s00603-024-03942-2.
[21] S. Ma, K. Liu, and J. Yang, *Investigation of blast-induced rock fragmentation and fracture characteristics with different decoupled charge structures*, Int. J. Impact. Eng. 185 (2024), pp. 104855. doi:10.1016/j.ijimpeng.2023.104855.
[22] M.B. Saka, S.O. Ayoola, and M.H.B.M. Hashim, *Investigating the impact of short burden and spacing on blasting output in Zeberced Quarry*, Appl. Mech. Mater. 918 (2024), pp. 59–64. doi:10.4028/p-wQQb0d.
[23] O. Omidi, Timing effects on fragmentation by blasting, [Master's thesis]. Queen's University, 2015.
[24] T.N. Hagan, The influence of controllable blast parameters on fragmentation and mining costs, *Proceedings of the 1st international symposium on rock fragmentation by blasting*, 1983, pp. 31–32.
[25] M. Hosseini, M. Khandelwal, R. Lotfi, and M. Eslahi, *Sensitivity analysis on blast design parameters to improve bench blasting outcomes using the Taguchi method*, Geomech. Geophys. Geo-Energ. Geo-Resour. 9 (1) (2023), pp. 9. doi:10.1007/s40948-023-00540-4.
[26] A. Agrawal, The effect of back rows delay timing and size of blast on fragmentation and muckpile shape parameter, [PhD diss]. Indian School of Mines, Dhanbad, 2013.
[27] S. Esen, H.A. Bilgin, and T. BoBo, Effect of explosive on fragmentation, *The 4th Drilling and Blasting Symposium*, *Ankara, Turkey*, Citeseer, 2000.
[28] M.S. Dotto and Y. Pourrahimian, *The influence of explosive and rock Mass properties on blast damage in a single-hole blasting*, Mining 4 (1) (2024), pp. 168–188. doi:10.3390/mining4010011.
[29] R.K. Paswan, M.P. Roy, R. Shankar, and P.K. Singh, *Blast vibration and fragmentation control at heavily jointed limestone mine*, Geotech Geol Eng 39 (5) (2021), pp. 3469–3485. doi:10.1007/s10706-021-01705-2.
[30] E. Marsh, J. Dahl, A.K. Pishhesari, J. Sattarvand, and F.C. Harris Jr, A virtual reality mining training simulator for proximity detection, *International Conference on Information Technology-New Generations*, Springer, 2023, pp. 387–393.
[31] J. van Eldert, H. Schunnesson, D. Johansson, and D. Saiang, *Application of measurement while drilling technology to predict rock mass quality and rock support for tunnelling*, Rock Mech Rock Eng 53 (3) (2020), pp. 1349–1358. doi:10.1007/s00603-019-01979-2.
[32] S. Manzoor. "*Predicting rock fragmentation based on drill monitoring: A case study from Malmberget mine, Sweden*, J. South. Afr. Inst. Min. Metall. 122 (3) (2022), pp. 1–11. doi:10.17159/2411-9717/1587/2022.
[33] M. Rodgers, M. McVay, D. Horhota, and J. Hernando, *Assessment of rock strength from measuring while drilling shafts in Florida limestone*, Can. Geotech. J. 55 (8) (2018), pp. 1154–1167. doi:10.1139/cgj-2017-0321.

[34] J. Navarro, H. Schunnesson, R. Ghosh, P. Segarra, D. Johansson, and J.Á. Sanchidrián, *Application of drill-monitoring for chargeability assessment in sublevel caving*, Int. J. Rock Mech. Min. Sci. 119 (2019), pp. 180–192. doi:10.1016/j.ijrmms.2019.03.026.
[35] S. Manzoor, S. Liaghat, A. Gustafson, D. Johansson, and H. Schunnesson, *Establishing relationships between structural data from close-range terrestrial digital photogrammetry and measurement while drilling data*, Eng. Geol. 267 (2020), pp. 105480. doi:10.1016/j.enggeo.2020.105480.
[36] P. Rai, H. Schunnesson, P.-A. Lindqvist, and U. Kumar, *Measurement-while-drilling technique and its scope in design and prediction of rock blasting*, Int. J. Min. Sci. Technol. 26 (4) (2016), pp. 711–719. doi:10.1016/j.ijmst.2016.05.025.
[37] B. Adebayo and B. Mutandwa, *Correlation of blast-hole deviation and area of block with fragment size and fragmentation cost*, Int. Res. J. Eng. Technol. (IRJET) 2 (7) (2015), pp. 402–406.
[38] J. Valencia, "*Blasthole location detection using support vector machine and convolutional neural networks on UAV images and photogrammetry models*, Electron. (Basel) 13 (7) (2024), pp. 1291. doi:10.3390/electronics13071291.
[39] A. Kamran-Pishhesari, A. Moniri-Morad, and J. Sattarvand, *Applications of 3D reconstruction in virtual reality-based teleoperation: A review in the mining industry*, Technol. (Basel) 12 (3) (2024), pp. 40. doi:10.3390/technologies12030040.
[40] S.A. Vokhmin, A.A. Kytmanov, G.P. Erlykov, E.V. Shevnina, G.S. Kurchin, and A.K. Kirsanov, *Prediction and actual Oversized/Undersized fragmentation in underground blasting*, J. Min. Sci 57 (2) (2021), pp. 210–219. doi:10.1134/S1062739121020058.
[41] B.O. Afum and V.A. Temeng, *Reducing drill and blast cost through blast optimisation–a case study*, Ghana Min. J. 15 (2) (2015), pp. 50–57.
[42] J.B. Ninepence, E.J.A. Appianing, B.A. Kansake, and R. Amoako, Optimisation of drill and blast parameters using emperical fragmentation modelling, *4th UMaT Biennial international mining and mineral conference*, 2016, pp. 25–299.
[43] L. Zhao, D. Su, Z. Li, B. Chen, R. Wang, and R. Chen, *Research on optimization of an open-bench deep-Hole blasting parameter using an improved Gray Wolf algorithm*, Appl. Sci. 14 (8) (2024), pp. 3514. doi:10.3390/app14083514.
[44] R. Battulwar, "*A practical methodology for generating high-resolution 3D models of open-pit slopes using UAVs: Flight path planning and optimization*, Remote Sens (Basel) 12 (14) (2020), pp. 2283. doi:10.3390/rs12142283.
[45] T. Kleine, P. Townson, and K. Riihioja, Assessment and computer automated blast design, *Proceedings of the 24th International Symposium on the Application of Computers and Operations Research in the Mineral Industries*, 1993, pp. 353–360.
[46] T. Pirinen, J. Lassila, M. Loimusalo, J. Pursimo, and S. Hanski, Automatic positioning and alignment for hole navigation in surface drilling, *The 31st International Symposium on Automation and Robotics in Construction and Mining (ISARC 2014)*, 2014, pp. 88–94.